Journal of Experimental Botany, Vol. 68, No. 2 pp. 321–333, 2017
doi:10.1093/jxb/erw417 Advance Access publication 18 November 2016
This paper is available online free of all access charges (see http://jxb.oxfordjournals.org/open_access.html for further details)

RESEARCH PAPER

Bundle-sheath leakiness and intrinsic water use efficiency of a perennial C_4 grass are increased at high vapour pressure deficit during growth

Xiao Ying Gong*, Rudi Schäufele and Hans Schnyder*

Lehrstuhl für Grünlandlehre, Technische Universität München, Alte Akademie 12, 85354 Freising, Germany

* Correspondence: xgong@wzw.tum.de and schnyder@wzw.tum.de

Received 27 June 2016; Editorial decision 20 October 2016; Accepted 20 October 2016

Editor: Susanne von Caemmerer, Australian National University

Abstract

Bundle-sheath leakiness (ϕ) is a key parameter of the CO_2-concentrating mechanism of C_4 photosynthesis and is related to leaf-level intrinsic water use efficiency (WUE_i). This work studied short-term dynamic responses of ϕ to alterations of atmospheric CO_2 concentration in *Cleistogenes squarrosa*, a perennial grass, grown at high (1.6 kPa) or low (0.6 kPa) vapour pressure deficit (VPD) combined with high or low N supply in controlled environment experiments. ϕ was determined by concurrent measurements of photosynthetic gas exchange and on-line carbon isotope discrimination, using a new protocol. Growth at high VPD led to an increase of ϕ by 0.13 and a concurrent increase of WUE_i by 14%, with similar effects at both N levels. ϕ responded dynamically to intercellular CO_2 concentration (C_i), increasing with C_i. Across treatments, ϕ was negatively correlated to the ratio of CO_2 saturated assimilation rate to carboxylation efficiency (a proxy of the relative activities of Rubisco and phosphoenolpyruvate carboxylase) indicating that the long-term environmental effect on ϕ was related to the balance between C_3 and C_4 cycles. Our study revealed considerable dynamic and long-term variation in ϕ of *C. squarrosa*, suggesting that ϕ should be determined when carbon isotope discrimination is used to assess WUE_i. Also, the data indicate a trade-off between WUE_i and energetic efficiency in *C. squarrosa*.

Key words: C_4 photosynthesis, CO_2-concentrating mechanism, carbon isotope discrimination, gas exchange, nitrogen nutrition, vapour pressure deficit.

Introduction

The CO_2 concentrating mechanism (CCM) is a specialized feature of C_4 photosynthesis and enables the maintenance of a very high CO_2 partial pressure at the site of ribulose-1,5-bisphosphate carboxylase/oxygenase (Rubisco), thus effectively minimizing photorespiration (Hatch, 1987). The CCM underlies the higher quantum yield, and higher water- and nitrogen-use efficiency of C_4 plants relative to C_3 plants under high temperature and/or low intercellular CO_2 (Ehleringer *et al.*, 1997; Long, 1999). In C_4 photosynthesis, CO_2 is first fixed by phosphoenolpyruvate carboxylase (PEPc) in mesophyll cells to form C_4 acids (the C_4 cycle), which are transported into bundle-sheath cells, where the acids are decarboxylated and CO_2 is finally fixed by Rubisco (the C_3 cycle). Effective CCM requires a strong 'CO_2 pump' (a high rate of the C_4 cycle). However, leakage of CO_2 from bundle-sheath cells back to mesophyll cells represents an energetic inefficiency that is

related to the cost of the regeneration of phosphoenolpyruvate (PEP; Hatch, 1987; Furbank *et al.*, 1990). The ratio of this leakage rate to the C_4 cycle rate is termed bundle-sheath leakiness (Farquhar, 1983), or leakiness (ϕ), and is a key parameter of C_4 photosynthesis.

Leakiness is generally quantified using a carbon isotope approach based on the model of carbon isotope discrimination (Δ) of C_4 photosynthesis (Farquhar, 1983). The simplified version of the C_4 discrimination model indicates that Δ is determined by ϕ and C_i/C_a, the ratio of intercellular CO_2 concentration (C_i) to atmospheric CO_2 concentration (C_a):

$$\Delta = a + (b_4 + \phi(b_3 - s) - a)C_i / C_a, \quad (1)$$

with a the fractionation during diffusion of CO_2 in air, b_4 the combined fractionation of PEP carboxylation and the preceding fractionation associated with dissolution of CO_2 and conversion to HCO_3^-, b_3 the fractionation by Rubisco and s the fractionation during leakage of inorganic C out of the bundle sheath. Since leaf-level intrinsic water use efficiency (WUE_i; net CO_2 assimilation rate/stomatal conductance) is a function of C_i and C_a, combined with Eqn 1 we have:

$$WUE_i = \frac{C_a}{1.6}\left(1 - \frac{\Delta - a}{b_4 + (b_3 - s)\phi - a}\right), \quad (2)$$

showing that WUE_i can be estimated from Δ if ϕ is known. Similar to the application of Δ to quantify WUE_i of C_3 plants (Farquhar and Richards, 1984; Yang *et al.*, 2016*b*), Δ was suggested as a potentially promising screening tool for breeding and improvement of C_4 crops (Henderson *et al.*, 1998; Gresset *et al.*, 2014; von Caemmerer *et al.*, 2014). However, such endeavours require knowledge of the magnitude and variability of ϕ and relevant environmental drivers. Early studies led to the notion that leakiness is relatively constant within a species with moderate short-term environmental variation, e.g. in response to light, CO_2, and temperature (Henderson *et al.*, 1992). A constant leakiness would largely simplify the relationship between WUE_i and Δ. However, more recent studies suggest dynamic variation of leakiness in response to short-term variation of irradiation (Kromdijk *et al.*, 2010; Pengelly *et al.*, 2010; Ubierna *et al.*, 2013; Bellasio and Griffiths, 2014) or temperature (von Caemmerer *et al.*, 2014).

Analysis of dynamic changes of leakiness in response to short-term variation of atmospheric CO_2 provides an opportunity for studying the functioning of the CCM. However, model analyses suggested an increase of leakiness with increasing C_i (von Caemmerer and Furbank, 1999; Kiirats *et al.*, 2002; Ghannoum, 2009; Yin *et al.*, 2011), while (the few) experimental studies using the carbon isotope approach showed no clear response of leakiness to C_i (Henderson *et al.*, 1992; Pengelly *et al.*, 2012).

Long-term effects of environmental drivers on leakiness have been observed. Thus, drought stress was shown to increase leakiness of several species (Saliendra *et al.*, 1996; Williams *et al.*, 2001; Fravolini *et al.*, 2002), and this effect was attributed to the relative activities of Rubisco/PEPc (Saliendra *et al.*, 1996). N stress was reported to affect leakiness of several sugarcane species (Meinzer and Zhu, 1998), but another study with different species found no effect of N fertilizer supply (Fravolini *et al.*, 2002). Increased CO_2 concentration was shown to increase (Watling *et al.*, 2000; Fravolini *et al.*, 2002) or have no effect (Williams *et al.*, 2001) on leakiness. Currently, it is unknown if vapour pressure deficit (VPD) during plant growth has an effect on leakiness. Studies on long-term effects of N nutrition, water supply, or CO_2 concentration during growth on leakiness using biomass-based Δ have considerable uncertainty related to post-photosynthetic fractionation and the temporal mismatch between biomass formation and gas exchange measurements as discussed by many authors (Henderson *et al.*, 1992; Cousins *et al.*, 2008; von Caemmerer *et al.*, 2014).

Scarcity of experimental evidence is partially due to the fact that quantifying leakiness using combined measurements of gas exchange and Δ ('on-line' Δ) is a laborious task. Measurement artefacts, i.e. CO_2 leak fluxes between the leaf cuvette and the surrounding air and isotopic disequilibria between photosynthetic and respiratory CO_2 fluxes, can lead to errors of measured Δ of several permil (Gong *et al.*, 2015). This technical issue is particularly relevant for C_4 species, as the Δ of C_4 plants is generally much lower than that of C_3 plants (Farquhar, 1983).

A previous study in our lab demonstrated that *Cleistogenes squarrosa* (Trin.) Keng—a perennial C_4 (NAD-ME) grass and co-dominant species in the semiarid steppe of Inner Mongolia—had a large and variable biomass-based Δ of leaves (6–9‰; Yang *et al.*, 2011), potentially indicating a high and variable ϕ. As ϕ is related to WUE_i (Eqn 2) and potentially driven by environmental factors, we were interested to unravel the mechanisms governing Δ in this C_4 species. Furthermore, understanding the physiological response of *C. squarrosa* to N nutrition and VPD may provide new insight into the adaptation of this species to its habitat given that: (i) water and N availability are the major limiting factors that determine primary production and resource use efficiency of plants in the semiarid steppes of Inner Monglia (Gong *et al.*, 2011) and (ii) the abundance of C_4 plants has increased substantially during the past several decades in the Mongolian plateau (Wittmer *et al.*, 2010). Given the lack of knowledge on long-term effects of VPD or N nutrition and short-term dynamic effects of CO_2 on ϕ, we performed controlled environment experiments with *C. squarrosa* grown under a low or high level of VPD combined with a low or high level of N fertilizer supply. Leakiness was determined using combined measurements of gas exchange and Δ (on-line Δ) following the protocols of Gong *et al.* (2015).

Materials and methods

Plant material and growth conditions

Cleistogenes squarrosa is an NAD-ME type (determined by ^{14}C labelling) C_4 grass, with a 'chloridoid' type of Kranz anatomy (Pyankov *et al.*, 2000). Stands of *C. squarrosa* were grown from seed in plastic pots (5 cm diameter, 35 cm depth) filled with quartz sand. Pots were placed in growth chambers (PGR15, Conviron, Winnipeg, Canada) at a density of 236 plants m^{-2}. A photosynthetic photon

flux density (PPFD) of 800 µmol m^{-2} s^{-1}, provided by cool white fluorescent tubes, was maintained at the top of the canopies during the 16 h-long photoperiods. Air temperature was maintained at 25 °C during photo- and dark periods. A CO_2 concentration ($[CO_2]$) of 386±3 µmol mol^{-1} (mean±SD, n>400) in chamber air was maintained during the photoperiods (cf. Schnyder *et al.*, 2003). A modified Hoagland nutrient solution was supplied three times per day by an automatic irrigation system throughout the entire experiment similar to Lehmeier *et al.* (2008). The time of first watering is referred to as imbibition of seeds. Before germination, all chambers were run with a VPD of 0.63 kPa (corresponding to a relative humidity (RH) of 80%).

N nutrition and VPD treatments

The study had a 2 × 2 factorial design, with N fertilizer supply and VPD as factors, two levels (low and high, see below) for each factor, and four replicates (four replicate stands) for each combination of N and VPD level. About 1 week after the imbibition of seeds (i.e. first watering), VPD and N treatment were implemented until the end of the experiment. The nutrient solution with 7.5 mM N in the form of equimolar concentrations of calcium nitrate and potassium nitrate was supplied to chambers of the low N treatment (N1), while another nutrient solution with 22.5 mM N was supplied to chambers of the high N treatment (N2). The concentration of other nutrients was the same in both nutrient solutions: 1.0 mM $MgSO_4$, 0.5 mM KH_2PO_4, 1 mM NaCl, 125 µM Fe-EDTA, 46 µM H_3BO_3, 9 µM $MnSO_4$, 1 µM $ZnSO_4$, 0.3 µM $CuSO_4$, 0.1 µM Na_2MoO_4. VPD (difference between actual vapour pressure and the saturation vapour pressure) was maintained at 0.63 kPa (corresponding to an RH of 80%) in the chambers of the low VPD treatment (V1) or at 1.58 kPa (corresponding to an RH of 50%) in the chambers of the high VPD treatment (V2). Each chamber (or each stand) was assigned to one of the treatments: N1V1, N1V2, N2V1, and N2V2. As we had a total of four chambers, in order to repeat each treatment four times, all replicates were accommodated in four sequential experimental runs (in total, 16 stands were grown) (cf. Table S1 in Liu *et al.* 2016). In each treatment, two replicate chambers were supplied with CO_2 from a mineral source ($\delta^{13}C_{CO_2}$ of −6‰) and the other two chambers with CO_2 from an organic source ($\delta^{13}C_{CO_2}$ of −33‰). Carbon isotope discrimination by the canopies led to some ^{13}C-enrichment of the CO_2 inside the growth chambers. However, that effect was small due to a high rate of air flow through the chambers: quasi-continuous on-line measurements of $\delta^{13}C_{CO_2}$ inside the growth chambers demonstrated a $\delta^{13}C_{CO_2}$ inside the chambers with the ^{13}C-enriched CO_2 source of −5.2±0.1‰ (mean±SD, n=23) and −31.7±0.1‰ (n=23) inside the chambers with the ^{13}C-depleted CO_2.

Gas exchange measurement system

The method reported by Gong *et al.* (2015) was used for leaf-level combined measurements of gas exchange and ^{13}C discrimination (on-line Δ). Measurements were performed using a leaf-level $^{13}CO_2/^{12}CO_2$ gas exchange and labelling system, which included a portable CO_2 exchange system (LI-6400, LI-COR Inc., Lincoln, NE, USA) housed in a gas exchange mesocosm (Gong *et al.*, 2015). The air supply to the mesocosm and LI-6400 was mixed from CO_2-free, dry air, and CO_2 of know $\delta^{13}C_{CO_2}$ (cf. Schnyder *et al.*, 2003). $[CO_2]$ inside the mesocosm (growth chamber) was monitored with an infrared gas analyser (LI-6262, LI-COR Inc.). During the measurement, the plant to be measured and the sensor head of the LI-6400 were placed inside the mesocosm, with concentration and $\delta^{13}C$ of CO_2 in both gas exchange facilities monitored and controlled. Using this set-up, we separately controlled the concentration and $\delta^{13}C$ in both facilities (sensor head and growth chamber) for purposes of gas exchange measurement or ^{13}C labelling (see below).

The mesocosm and leaf cuvette systems were coupled to a continuous-flow isotope ratio mass spectrometer (IRMS; Delta^{plus} Advantage equipped with GasBench II, ThermoFinnigan, Bremen, Germany) via a stainless steel capillary. Sample air was drawn through the capillary via a peristaltic pump and passed through a 0.25 ml sample loop attached to the 8-port Valco valve of the GasBench II. Sample air in the loop was introduced into the IRMS via an open split after passage of a dryer (Nafion) and a GC column (25 m×0.32 mm Poraplot Q; Chrompack, Middleburg, The Netherlands). After every second sample a VPDB-gauged CO_2 reference gas was injected into the IRMS via the Open Split. The whole-system precision (SD) of repeated measurements was 0.10‰ (n=50). For further details of the method see Gong *et al.* (2015).

Gas exchange and concurrent on-line ^{13}C discrimination measurements

Gas exchange and on-line Δ measurements followed the optimized protocols suggested by Gong *et al.* (2015). In order to minimize the effects of any CO_2 leak artefact across the gaskets of the clamp-on leaf cuvette and the surrounding (mesocosm) air, $[CO_2]$ inside the mesocosm was maintained close to that of the leaf cuvette of the LI-6400 (with the difference <30 µmol mol^{-1}), and the same CO_2 source was supplied to the mesocosm and LI-6400. By these means, the diffusive gradient of $^{13}CO_2$ or $^{12}CO_2$ between leaf cuvette and the surrounding air was effectively minimized (Gong *et al.*, 2015). In order to also minimize the isotopic disequilibrium artefact between the photosynthetic and respiratory CO_2 flux, the same CO_2 source was used for growing plants and for on-line leaf-level Δ measurements (Gong *et al.*, 2015).

Gas exchange and on-line Δ measurements were performed on the fully expanded young leaves near the tip of major tillers (the second youngest fully expanded leaf), started at about 38 days and ended at about 53 days after the imbibition of seeds. We used the standard 2 × 3 cm cuvette of LI-6400. Two leaf blades from separate major tillers of the same plant were carefully placed in the cuvette. This was done to compensate for the narrow leaf width of *C. squarrosa* (about 3 mm). The enclosed leaf area was determined after gas exchange measurements by photographing the leaf blades and analysis with ImageJ software (National Institutes of Health, Bethesda, MD, USA). All gas exchange parameters were recomputed using the measured enclosed leaf area.

Photosynthetic CO_2 response curves were taken with the successive CO_2 steps of 390, 800, 390, 260, 180, 120, 90, 60, and 30 µmol mol^{-1} ($[CO_2]$ in the cuvette) on at least two plants randomly chosen from each growth chamber. In total, 42 plants were measured. The data of five plants were eliminated from further analysis due to extremely low leaf N contents. Finally, each treatment had nine to ten replicates of individual plants. During the gas exchange measurements, the environmental parameters were maintained close to the growth conditions: leaf temperature was maintained at 25 °C, PPFD at 800 µmol m^{-2} s^{-1}, leaf-to-air VPD at 0.76–0.96 kPa (V1 treatment) or 1.4–1.6 kPa (V2 treatment; Supplementary Fig. S1 at *JXB* online) at all CO_2 levels. To generate the appropriate VPD for gas exchange measurements, the inflow air stream (well-mixed dry air) was passed through a gas washing bottle placed in a temperature-controlled water bath. For each step of the CO_2 response, the $[CO_2]$ in the mesocosm was also adjusted to be close to that of the cuvette. Leaves were acclimated for at least 30 min before the start of gas exchange measurements. After CO_2 exchange rates reached a steady state at each step of the CO_2 response, gas exchange parameters (measured by LI-6400), e.g. net CO_2 assimilation rate (A), transpiration rate (E), and stomatal conductance to vapour (g_s) were recorded. Instantaneous water use efficiency was calculated as $WUE_{ins}=A/E$; intrinsic water use efficiency was calculated as $WUE_i=A/g_s$.

Among the 37 CO_2 response curves, 22 plants were concurrently measured for on-line ^{13}C discrimination. For this, the $[CO_2]$ and $\delta^{13}C$ of the incoming (C_{in} and δ_{in}) and outgoing cuvette air (C_{out} and δ_{out}) were measured on five to six plants per treatment combination. All measurements of $\delta^{13}C$ were corrected for the non-linearity effect of the IRMS (Elsig and Leuenberger, 2010).

^{13}C discrimination during net CO_2 assimilation (Δ) was calculated according to Evans *et al.* (1986):

$$\Delta = \frac{\xi(\delta_{out} - \delta_{in})}{1 + \delta_{out} - \xi(\delta_{out} - \delta_{in})}, \quad (3)$$

where $\xi = C_{in}/(C_{in} - C_{out})$.

Determination of leaf respiration rate in light

Additional measurements were performed to determine leaf respiration rate in light (R_L). This was done with leaves of the same age class as used for CO_2 response measurements using the ^{13}C labelling method reported by Gong *et al.* (2015). All measurements were performed under growth conditions (i.e. at C_a of 390 μmol mol^{-1}, PPFD of 800 μmol m^{-2} s^{-1}). Briefly, Δ of each leaf was measured first with the same CO_2 source as used for growing plants, then the same measurement was repeated with the other CO_2 source (i.e. the ^{13}C-enriched or -depleted CO_2 source). Making use of isotopic disequilibria between photosynthetic and respiratory CO_2 fluxes derived from the two sets of on-line Δ measurements, the ratio of R_L to net CO_2 assimilation rate (A) was solved as:

$$R_L / A = (\delta_{AE} - \delta_{AD}) / (\delta_{outE} - \delta_{outD}) - 1, \quad (4)$$

$$\delta_A = (\delta_{in} C_{in} - \delta_{out} C_{out}) / (C_{in} - C_{out}), \quad (5)$$

where δ_A and δ_{out} are the $\delta^{13}C$ of net CO_2 assimilation and that of CO_2 in the cuvette, respectively, and subscripts E and D indicate the relevant parameters measured with the ^{13}C-enriched or the ^{13}C-depleted sources of CO_2, respectively. R_L was measured on six individuals in each treatment. R_L of other leaves of the same treatment was estimated by multiplying A of that leaf by the treatment-specific mean of R_L/A. For further details of the methodology see Gong *et al.* (2015).

Bundle-sheath leakiness (ϕ), C_3 cycle rate and C_4 cycle rate

Bundle-sheath leakiness was determined using the complete version of the Farquhar C_4 discrimination model (Farquhar, 1983), modified to include the ternary correction (Farquhar and Cernusak, 2012):

$$\Delta = \frac{1}{1-t}\left[a_b \frac{C_a - C_L}{C_a} + a \frac{C_L - C_i}{C_a}\right] + \frac{1+t}{1-t}\left[(e_s + a_l)\frac{C_i - C_m}{C_a} + \frac{b_4 + \phi\left(\frac{b_3 C_{bs}}{C_{bs} - C_m} - s\right)}{1 + \frac{\phi C_m}{C_{bs} - C_m}} \frac{C_m}{C_a}\right], \quad (6)$$

where C_a, C_L, C_i, C_m, and C_{bs} are the CO_2 concentrations in air ($C_a = C_{out}$ during gas exchange measurements), at the leaf surface, in the intercellular airspace, in the mesophyll cell, and in the bundle-sheath cell, respectively. C_L was calculated as $C_L = C_a - 1.37A/g_{BL}$, with g_{BL} the boundary layer conductance to vapour calculated by the LI-6400 software. a_b=2.9‰, a=4.4‰, e_s=1.1‰, a_l=0.7‰, and s=1.8‰ denote fractionation constants associated with CO_2 diffusion across boundary layer, across stomata, dissolution in water, diffusion in liquid phase, and leaking out of bundle sheath cells, respectively. t represents the ternary correction factor (Farquhar and Cernusak, 2012):

$$t = (1 + \bar{a}) E / (2 g_{sc}), \quad (7)$$

where E is the transpiration rate and g_{sc} is the total conductance to CO_2: $g_{sc} = 1/(1.6/g_s + 1.37/g_{BL})$, where g_s is the stomatal conductance to vapour. $\bar{a}$ is the weighted fractionation across boundary layer (a_b=2.9‰) and stomata (a=4.4‰): $\bar{a} = [a_b(C_a - C_L) + a(C_L - C_i)]/(C_a - C_i)$. b_3 (^{13}C fractionation during carboxylation by Rubisco including respiratory fractionation) and b_4 (^{13}C fractionation by CO_2 dissolution, hydration, and PEPc carboxylation including respiratory fractionation) were calculated according to Farquhar (1983):

$$b_3 = b'_3 - eR_L / V_c - 0.5 f V_o / V_c, \text{ and} \quad (8)$$

$$b_4 = b'_4 - 0.5 e R_L (1 - \phi) / (A + 0.5 R_L), \quad (9)$$

where b'_3=30‰, b'_4=–5.7‰, e=–6‰ (Ghashghaie *et al.*, 2003; Kromdijk *et al.*, 2010), f=11.6‰ (Ghashghaie *et al.*, 2003; Lanigan *et al.*, 2008), and V_c is the rate of Rubisco carboxylation and V_o is the rate of oxygenation. In our experiments, the same source CO_2 was used for growing plants and for online Δ measurements; therefore an additional term (cf. e' in Ubierna *et al.* 2013) accounting for the discrepancy of $\delta^{13}C_{CO_2}$ between growth environment and gas exchange measurements was not included. Here, it is assumed that respiration in mesophyll cells (R_m) and bundle-sheath cells (R_{bs}) both equal $0.5R_L$ (von Caemmerer and Furbank, 1999; Pengelly *et al.*, 2010).

To solve ϕ using Eqns 7–9, C_m, C_{bs}, V_o, and V_c must be estimated. Those parameters were determined using the equations of the C_4 photosynthesis model of von Caemmerer and Furbank (1999). C_m can be calculated from:

$$g_m = A / (C_i - C_m), \quad (10)$$

if mesophyll conductance to CO_2 is known. It has been generally assumed that g_m is high and non-limiting for CO_2 assimilation in C_4 photosynthesis. Thus, in many published works on ϕ, g_m was assumed to be infinite, i.e. $C_i = C_m$. However, a recent study using a new oxygen isotope approach found that g_m of C_4 species ranged between 0.66 and 1.8 mol m^{-2} s^{-1} measured at a leaf temperature of about 32 °C (Barbour *et al.*, 2016). We calculated the minimum g_m as: $g_{mmin} = A/C_i$ (von Caemmerer *et al.*, 2014). These results showed that g_{mmin} decreased with increasing C_i (see Supplementary Fig. S2). Further, we assumed that the young leaves of *C. squarrosa* had a g_m of 0.66 mol m^{-2} s^{-1} at the growth C_a of 390 μmol mol^{-1}. Appling a constant ratio of g_m/g_{mmin} across the CO_2 response curve, we estimated the response of g_m to C_i. The estimates of g_m ranged between 0.2 and 2.4 mol m^{-2} s^{-1} and decreased with increasing C_i (Supplementary Fig. S2); similarly, decrease of g_m with increasing C_i was found in other C_4 species using the oxygen isotope approach (Osborn *et al.*, 2016) or an '*in vitro* V_{pmax}' method (N. Ubierna, personal communication).

A simplified version of the C_4 photosynthesis model for enzyme-limited CO_2 assimilation rate (von Caemmerer and Furbank, 1999) can be used to model the photosynthetic CO_2 response curve: $A = \min[(V_p - R_m + g_{bs} C_m), (V_{cmax} - R_L)]$, where V_P is the rate of PEP carboxylation, V_{cmax} is the maximum rate of Rubisco carboxylation, and g_{bs} is the bundle-sheath conductance to CO_2. A is determined by the term $V_{cmax} - R_L$ at high CO_2 concentrations. According to this model, we assumed that $V_{cmax} = A_{max} + R_L$, where A_{max} is the maximum net assimilation rate observed in the photosynthetic light response curves measured on leaves of the same age at ambient CO_2 (data shown in Supplementary Fig. S3). Treatment-specific V_{cmax} of *C. squarrosa* ranged between 16 and 19 μmol m^{-2} s^{-1}, which is in the range of V_{cmax} of C_4 grass used in Earth System Models (13–33 μmol m^{-2} s^{-1}; Rogers, 2014). C_{bs} was estimated using equations of von Caemmerer and Furbank (1999):

$$C_{bs} = \frac{\gamma^* O_{bs} + K_c\left(1 + \frac{O_{bs}}{K_o}\right)(A + R_L)/V_{cmax}}{1 - (A + R_L)/V_{cmax}}, \quad (11)$$

$$O_{bs} = \alpha A / (0.047 g_{bs}) + O_m, \quad (12)$$

where O_{bs} is the bundle-sheath oxygen concentration, and O_m (210 mmol mol^{-1}) is the oxygen concentration in mesophyll cells; γ^* (0.000193) is half of the reciprocal of Rubisco specificity; K_c and K_o are the Michaelis–Menten constants of Rubisco for CO_2 (650 μmol mol^{-1}) and O_2 (450 μmol mol^{-1}) at 25 °C, respectively; α (0.1) is the fraction of PSII activity in the bundle-sheath; g_{bs}=0.003 mol m^{-2} s^{-1}. Furthermore, V_o/V_c was calculated as $V_o/V_c = 2\gamma^* O_{bs}/C_{bs}$. Knowing V_o/V_c, V_o and V_c were calculated using the equation: $V_c = A + R_L + 0.5V_o$. The values of model parameters and equations were derived from von Caemmerer and Furbank (1999). Knowing ϕ and applying the assumption that $R_m = R_{bs} = 0.5R_L$ (von Caemmerer and Furbank, 1999; Pengelly *et al.*, 2010), the rate of PEP carboxylation (V_p) or Rubisco carboxylation (V_c) was estimated (see Supplementary Fig. S4). As C_m and C_{bs} cannot be directly measured, the determination of both parameters in this study was associated with some uncertainty. Another commonly used assumption in calculating leakiness using the complete or simplified version of Eqn 6 is that CO_2 is in equilibrium with HCO_3^- in the mesophyll cytoplasm. The extent of this equilibrium is determined by the relative rate of PEP carboxylation and hydration of CO_2 (V_h). If CO_2 is not in equilibrium with HCO_3^-, b'_4 of –5.7‰ in Eqn 9 should be replaced by $b'_4 = -5.7 + 7.9V_p/V_h$ (Farquhar 1983). Thus, we calculated ϕ using C_4 discrimination models with different assumptions on g_m, C_{bs}, and V_p/V_h (Supplementary Fig. S5). These results are compared and discussed below.

Fitting of CO_2 response curves

For each plant, measured A was plotted against the respective intercellular CO_2 concentration. A model of C_4 photosynthesis was used to fit the CO_2 response curves (Wang *et al.*, 2012):

$$A = a'(1 - e^{-b'x}) + c' \quad (13)$$

where x is C_i and c' is R_L. Using the fitted parameters (a' and b') of each CO_2 response curve, CO_2-saturated net assimilation rate (A_{sat}) was obtained as ($a'+c'$), and carboxylation efficiency (CE) was calculated as $b'(a'+c')$ (the initial slope of the A–C_i curve). For CO_2 response curves of C_4 leaves, A_{sat} is proportional to Rubisco activity, while CE is proportional to the PEP carboxylase activity (von Caemmerer and Furbank, 1999; Yin *et al.*, 2011). The ratio of A_{sat} to CE was calculated to indicate the ratio of Rubisco to PEPc activities.

Leaf trait parameters and nitrogen nutrition index

N content in dry mass of leaves previously used for gas exchange measurements was measured using an elemental analyser (NA 1110, Carlo Erba, Milan, Italy). For sample preparation, leaves were dried at 60 °C for 48 h, weighed and then milled. N content on a mass (N_{mass}, %DM) and leaf area basis (N_{area}, g m^{-2}) were calculated. Specific leaf area (SLA, cm^2 mg^{-1}) was obtained as SLA=leaf area/leaf dry mass. In each experiment, a set of individual plants (four plants per chamber) were sampled four or five times (twice per week) after canopy closure (when leaf area index was >2) for the determination of standing aboveground biomass, and N content in total aboveground dry mass. Those data were used to calculate nitrogen nutrition index (NNI) according to Lemaire *et al.* (2008).

Statistical analysis

Two-way ANOVA was used to test the effects of N supply, VPD, and their interactions on leaf traits and gas exchange parameters, using general linear models of SAS (SAS 9.1, SAS Institute, USA). The effects of N nutrition and VPD on the relationship between lnC_i and leakiness were analysed using a dummy regression approach; the parallelism and coincidence of linear regressions of different treatments were tested according to Berenson *et al.* (1983). Non-linear regression analysis on photosynthetic CO_2 response curve of individual plants was performed using the Nlin procedure of SAS.

Results

Leaf traits and photosynthetic CO_2 assimilation

N supply increased N_{mass} of fully expanded young leaves by 25% (P<0.05) and also tended to increase N_{area} (P=0.06), but had no effect on SLA (Table 1). N supply also significantly increased

Table 1. *Leaf trait and gas exchange parameters of* C. squarrosa *measured under the same environmental conditions as during growth (leaf temperature 25 °C, PPFD 800 μmol m^{-2} s^{-1}, [CO_2] 390 μmol mol^{-1}, VPD 0.8 kPa for V1 and 1.6 kPa for V2)*

Plants were grown at low or high N fertilizer supply (N1 or N2) combined with low or high VPD (V1 or V2). Leaf trait parameters include N content per unit dry mass (N_{mass}, % DM) and per leaf area (N_{area}, g m^{-2}), and specific leaf area (SLA, cm^2 mg^{-1}). Gas exchange parameters: net CO_2 assimilation rate (A, μmol m^{-2} s^{-1}), transpiration rate (E, mmol m^{-2} s^{-1}), stomatal conductance to water vapor (g_s, mol m^{-2} s^{-1}), respiration rate in light (R_L, μmol m^{-2} s^{-1}), the ratio of internal to atmospheric CO_2 concentration (C_i/C_a), instantaneous water use efficiency (WUE_{ins}=A/E, mmol mol^{-1}), and intrinsic water use efficiency (WUE_i=A/g_s, μmol mol^{-1}). Data are shown as mean±SE (n=6 for R_L, n=9–10 for the other parameters). Significant treatment effects (P<0.05) are shown in bold.

	N1		N2		*P*-value		
	V1	V2	V1	V2	N	VPD	N×VPD
N_{mass}	2.4 ± 0.1	2.4 ± 0.1	3.0 ± 0.1	3.0 ± 0.2	**0.01**	0.81	0.79
N_{area}	1.2 ± 0.2	1.3 ± 0.2	1.6 ± 0.2	1.6 ± 0.2	0.06	0.82	0.92
SLA	0.21 ± 0.02	0.20 ± 0.02	0.21 ± 0.02	0.21 ± 0.02	0.91	0.82	0.85
A	14.8 ± 0.9	13.1 ± 0.9	14.9 ± 0.9	12.3 ± 1.0	0.81	**0.03**	0.58
E	0.93 ± 0.08	1.14 ± 0.09	0.93 ± 0.08	1.23 ± 0.09	0.69	**0.01**	0.60
g_s	0.10 ± 0.01	0.08 ± 0.01	0.11 ± 0.01	0.07 ± 0.01	0.69	**0.01**	0.45
R_L	0.81 ± 0.26	0.62 ± 0.30	0.53 ± 0.10	0.51 ± 0.10	0.36	0.62	0.71
C_i/C_a	0.35 ± 0.03	0.26 ± 0.04	0.35 ± 0.03	0.25 ± 0.04	0.93	**0.01**	0.91
WUE_{ins}	15.9 ± 0.6	11.7 ± 0.6	16.8 ± 0.6	10.0 ± 0.6	0.82	**0.01**	**0.04**
WUE_i	153 ± 9	173 ± 9	154 ± 9	178 ± 10	0.79	**0.02**	0.82

nitrogen nutrition index (NNI; determined from N content and aboveground standing biomass of each stand): NNI was 0.88 ± 0.05 (mean±SD, n=4 replicate stands) for the N1V1 treatment, 0.71±0.06 for the N1V2 treatment, 1.25±0.06 for the N2V1 treatment, and 1.32±0.05 for the N2V2 treatment. The effects of VPD and the interaction of VPD and N supply on N_{mass}, N_{area} and SLA were all non-significant (P>0.05) (Table 1).

The effects of N supply on N_{mass} and N_{area} were not associated with parallel effects on gas exchange parameters measured at growth CO_2 level (390 μmol mol^{-1}). Thus, N supply had no effect on A, E, g_s, C_i/C_a, and WUE_{ins}, and there was only a small interactive effect of N and VPD on WUE_i (Table 1). Conversely, VPD during growth had significant effects on all these parameters, but none of these effects demonstrated an interaction with N supply except for WUE_{ins}. High VPD decreased A by 14%, g_s by 29%, C_i/C_a by 27% at both low and high N, and WUE_{ins} by 26% at low N and 40% at high N. Conversely, high VPD increased E by 27% and WUE_i by 14% independently of N levels (Table 1). The rate of leaf respiration in light (R_L) did not differ between treatments.

The response of photosynthetic gas exchange parameters to dynamic changes of CO_2 concentration (Fig. 1) showed typical CO_2 responses of net CO_2 assimilation rate. VPD had clear effects on gas exchange parameters: compared with low VPD, A was 20% lower (Fig. 1A, B), E was 21% higher (Fig. 1C, D), and g_s was 32% lower (Fig. 1E, F) at high VPD averaged over N levels and CO_2 concentrations.

Carbon isotope discrimination and bundle-sheath leakiness

Carbon isotope discrimination (Δ) during net CO_2 exchange revealed strong dynamic responses to short-term variation of CO_2 concentration; Δ increased with increasing C_i in all treatments, and ranged from 4 to 8‰ (Fig. 2A, B). Compared at the same C_i, Δ was higher at high VPD than at low VPD. Estimates

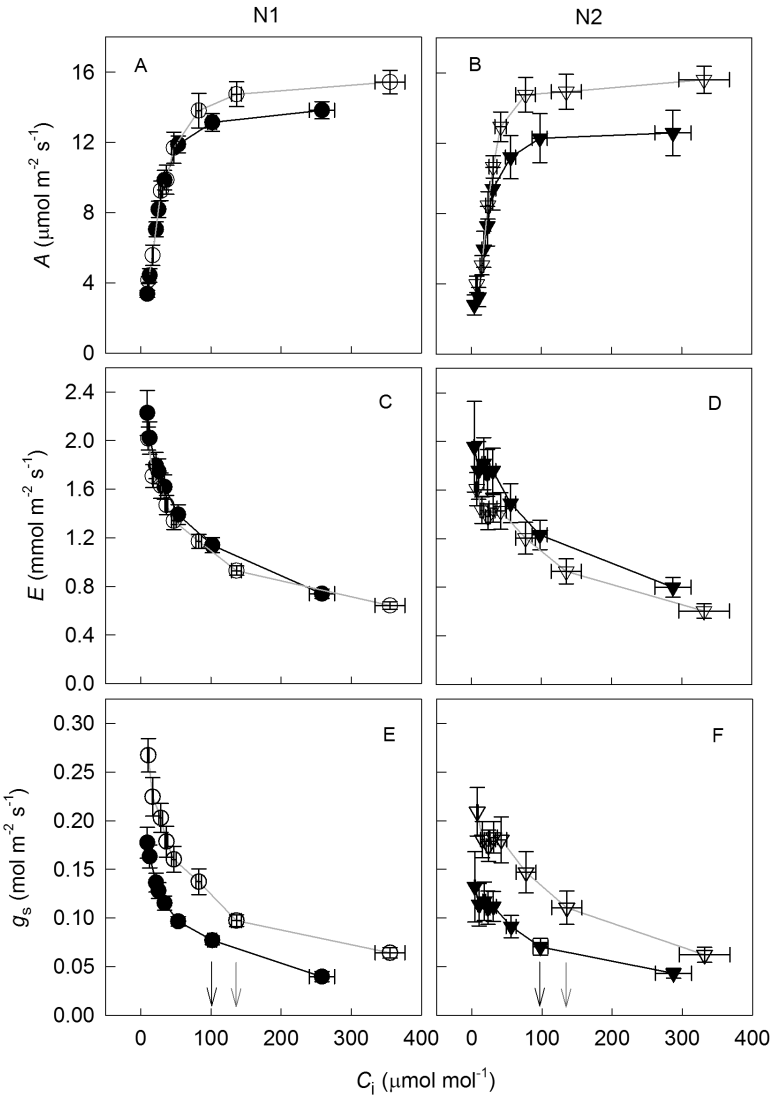

Fig. 1. Net CO_2 assimilation rate (A; A, B), transpiration rate (E; C, D) and stomatal conductance to water vapour (g_s; E, F) in response to short-term variation of intercellular CO_2 (C_i) under low (N1, circles; A, C, E) or high N supply (N2, triangles; B, D, F) combined with low (V1, open symbols) or high VPD (V2, filled symbols). Data are shown as the mean±SE (n=9–10). Operating conditions of gas exchange measurements were the same as conditions in growth chambers (leaf temperature 25 °C, PPFD 800 μmol m^{-2} s^{-1}, VPD 0.8 kPa for V1 and 1.6 kPa for V2). The corresponding C_i values at growth CO_2 concentration (390 μmol mol^{-1}) are indicated by grey (low VPD) and black arrows (high VPD) in (E) and (F).

of ϕ also increased with increasing C_i in all treatments, and ranged from 0.23 to 0.81 (Fig. 2C, D). The relationship between C_i and ϕ followed a logarithmic function. Regression analyses between lnC_i and ϕ including VPD as a dummy variable indicated a significant VPD effect on ϕ: ϕ was higher by 0.13 at high VPD than at low VPD at both N levels (Fig. 3, Table 2). Plants grown with high N supply had a higher ϕ at moderate to low C_i (C_a≤390) than plants with low N supply (Fig. 3). Accordingly, the slope of the linear regression between lnC_i and ϕ was significantly lower for the high N treatment than for the low N treatment (Table 2). The increase of ϕ along the gradient of C_i was apparently related to the discrepancy between rates of C_3 and C_4 cycles: V_c already reached the maximum at a C_i<100 μmol mol^{-1}, while V_p increased throughout the range of measured C_i (Supplementary Fig. S4). We also calculated ϕ using C_4 discrimination models with different assumptions on g_m, C_{bs}, and V_p/V_h, and our conclusions on short-term response to CO_2 and long-term response to VPD and N were not altered (see Supplementary Fig. S5).

Relationships between leaf traits and gas exchange parameters

VPD had a clear effect on A_{sat} (Fig. 4A): averaged over N treatments, high VPD caused a 15% reduction of A_{sat}. N supply and N×VPD interactions had no effect on A_{sat}. CE of leaves seemed to be slightly higher at high (0.71 mol m^{-2} s^{-1}) than low N (0.53 mol m^{-2} s^{-1}), although this effect was only significant at P=0.10 (Fig. 4B). A_{sat}/CE was calculated to indicate the ratio of Rubisco to PEPc activities. Treatment-specific mean A_{sat}/CE was negatively correlated with ϕ (P<0.05, Fig. 4C). Across all treatments, we found no correlation between A_{sat} and N_{mass} (P=0.41, Fig. 5A), but a positive correlation between CE and N_{mass} (r^2=0.43, P<0.001, Fig. 5B) and a negative correlation between A_{sat}/CE and N_{mass} (r^2=0.29, P<0.001, Fig. 5C). WUE_i was negatively correlated with A_{sat} (r^2=0.34, P<0.001, Fig. 6A) and A_{sat}/CE (r^2=0.49, P<0.001, Fig. 6C), but positively with CE (r^2=0.19, P<0.001, Fig. 6B) and leakiness (r^2=0.19, P<0.05, Fig. 6D). Furthermore, a positive correlation between WUE_i and leakiness was also found during short-term response to CO_2 (r^2>0.9, P<0.01, Supplementary Fig. S6).

Discussion

This study indicates an effect of VPD of the growth environment on bundle-sheath leakiness: ϕ was higher at high VPD than at low VPD with an absolute difference of 0.13 at both N supply levels. This effect appeared to be constitutive,

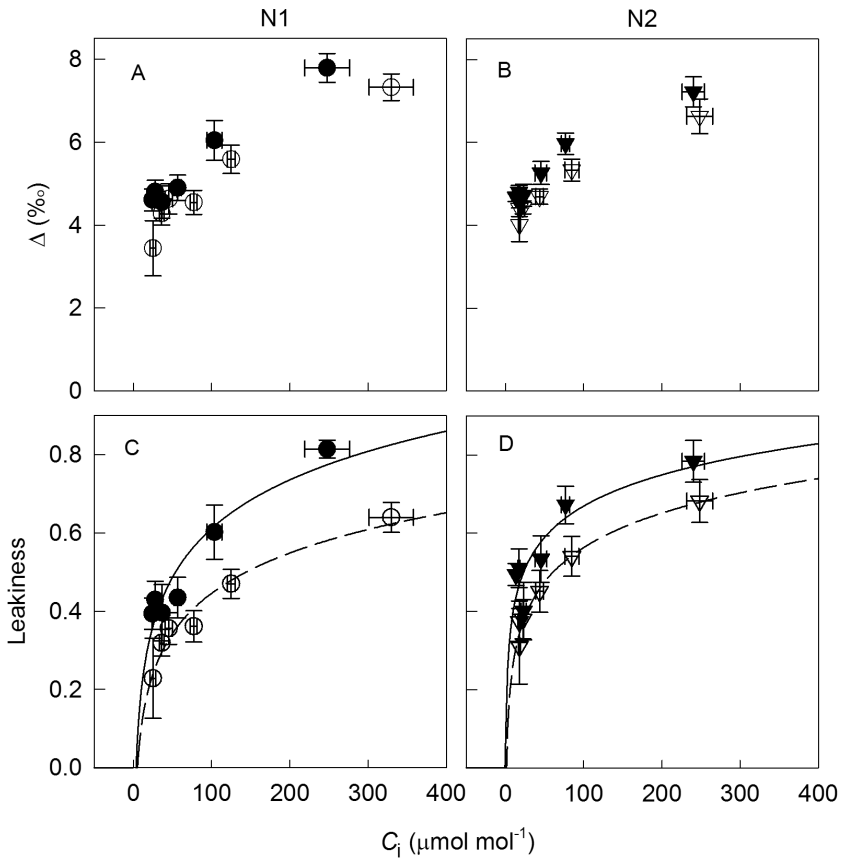

Fig. 2. Carbon isotope discrimination (Δ) during net CO_2 exchange (A, B) and bundle sheath leakiness (C, D) of *Cleistogenes squarrosa* leaves in response to short-term variation of intercellular CO_2 (C_i). Plants were grown under low (N1, circles; A, C) or high N supply (N2, triangles; B, D) combined with low (V1, open symbols, dashed lines) or high VPD (V2, filled symbols, solid lines). Operating conditions of gas exchange measurements were the same as conditions in growth chambers (leaf temperature 25 °C, PPFD 800 μmol m^{-2} s^{-1}, VPD 0.8 kPa for V1 and 1.6 kPa for V2). Data are shown as the mean±SE (n=5–6). The regressions were fitted using a function of $y=y_0+a\ln(x)$; all regressions have r^2>0.8.

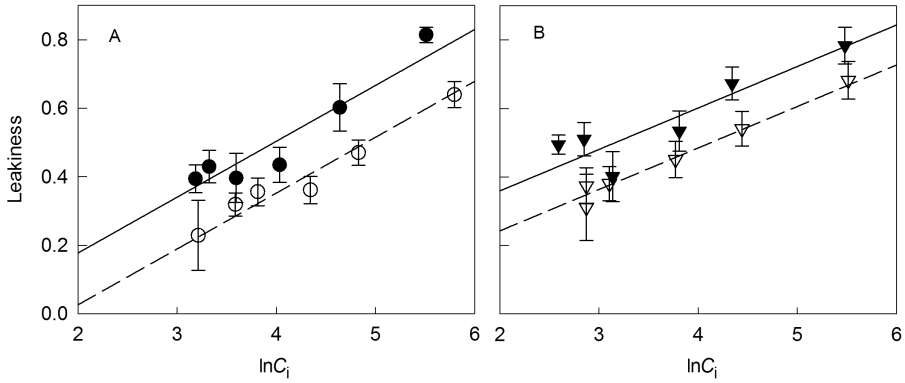

Fig. 3. Relationships between bundle sheath leakiness and ln(C_i) under low (N1, circles; A) or high N supply (N2, triangles; B) combined with low (V1, open symbols, dashed lines) or high VPD (V2, filled symbols, solid lines). Operating conditions of gas exchange measurements were the same as conditions in growth chambers (leaf temperature 25 °C, PPFD 800 μmol m^{-2} s^{-1}, VPD 0.8 kPa for V1 and 1.6 kPa for V2). Data are shown as the mean±SE (n=5–6). The data of each N level were fitted by linear regression including a dummy variable indicating VPD treatments (V) after the confirmation of parallelism of the two regressions of VPD levels: with V=0 for low VPD and V=1 for high VPD (for equations see Table 2).

Table 2. *Results of regression analysis on the relationship between C_i and leakiness (ϕ)*

The data for each N level were fitted by linear regression including a dummy variable indicating VPD treatments (V) after the confirmation of parallelism of the two regressions of VPD levels, with V=0 for low VPD and V=1 for high VPD; 95% confidence intervals of slope and coefficient of dummy variable (V) are shown. The coefficient of V quantifies the mean difference in ϕ between high and low VPD treatments across C_i levels. Both regressions are significant (P<0.001).

N level	equation	r^2	95% CI slope	95% CI coeff. V
N1	ϕ=−0.30+0.16lnC_i+0.15V	0.94	0.13~0.20	0.09~0.21
N2	ϕ=0.001+0.12lnC_i+0.12V	0.91	0.09~0.15	0.05~0.18

as it was manifest throughout a wide range of short-term variations of CO_2 concentration. Remarkably, the higher leakiness at high VPD was associated with a 14% improved WUE_i. Also, we observed an N effect on ϕ that responded to short-term variation of CO_2 levels: high N supply increased ϕ of leaves at ambient to low CO_2 levels (C_a≤390 μmol mol^{-1}). Further, ϕ responded dynamically to short-term changes of [CO_2], in support of theoretical predictions of C_4 photosynthesis models (von Caemmerer and Furbank, 1999; Yin *et al.*, 2011). Lastly, across treatments, a positive correlation between WUE_i and leakiness was evident, pointing to a trade-off between WUE_i and energy use efficiency of this species.

Unfortunately, leakiness cannot be measured directly, and the online $\Delta^{13}C$ approach for estimations of leakiness in conjunction with the C_4 photosynthetic discrimination model of Farquhar (1983) can lead to inaccurate estimates of leakiness if improper simplifications are made (Ubierna *et al.*, 2011, 2013; Gong *et al.*, 2015). One commonly used assumption is that g_m of C_4 plants is infinite, and thus C_i=C_m. However, a recent study indicated that g_m of C_4 plants is finite, although close to the high-end values of g_m of C_3 plants (Barbour *et al.*, 2016). In our study, assuming a lower range of g_m across C_i levels (see Supplementary Fig. S5), or a constant g_m of 1.8 mol m^{-2} s^{-1} (data not shown) or an infinite g_m (Supplementary Fig. S5) did not modify observed treatment effects. Only if g_m was much lower at low compared with high VPD (e.g. g_m at N1V1 was 60% lower than at N1V2 treatment), would VPD effects on leakiness disappear. However, it is unlikely that *C. squarrosa* had lower g_m at low than at high VPD, as studies with C_3 species generally showed a decrease of g_m by high VPD or water stress (Flexas *et al.*, 2008). Thus, our estimates of treatment effects on leakiness appeared to be largely insensitive to assumptions on g_m.

Many studies using Eqn 6 have assumed that CO_2 is in equilibrium with HCO_3^- in the mesophyll cytoplasm. However, according to Cousins *et al.* (2008) that assumption might not be proper, especially for C_4 grasses, which have lower carbonic anhydrase (CA) activity than C_4 dicots. Our observations with the same species in the same experiment suggested that, under growth conditions, assimilated CO_2 was in equilibrium with HCO_3^-, as indicated by the fact that $\delta^{18}O$ of leaf cellulose did not differ between plants growing in the presence of CO_2 with contrasting $\delta^{18}O$ (Liu *et al.*, 2016). Thus the observed treatment effects on leakiness of *C. squarrosa* seemed not to be related to CA activity. Further, we calculated leakiness using different assumptions on V_p/V_h: V_p/V_h=0 or V_p/V_h=0.23 (mean of NAD-ME grasses in Cousins *et al.*, 2008) and observed a minor effect on leakiness (less than 0.06). Thus, the short-term response of leakiness to CO_2 was not explained by changes in V_p/V_h. Applying another commonly used simplification that C_{bs} is sufficiently higher than C_m, so that $C_{bs}/(C_{bs}-C_m)$=1 and $C_m/(C_{bs}-C_m)$=0, also had no influence on our conclusions on effects of environmental factors on leakiness.

Effects of VPD and N nutrition on bundle-sheath leakiness

The study demonstrated a higher leakiness of plants grown at high VPD than at low VPD, and this effect was not modified by N nutrition. The present effect was not related to drought stress, as the elongation rate of phytomers (Yang *et al.*, 2016*a*) and the growth rate of individuals (Liu *et al.*, 2016) were not

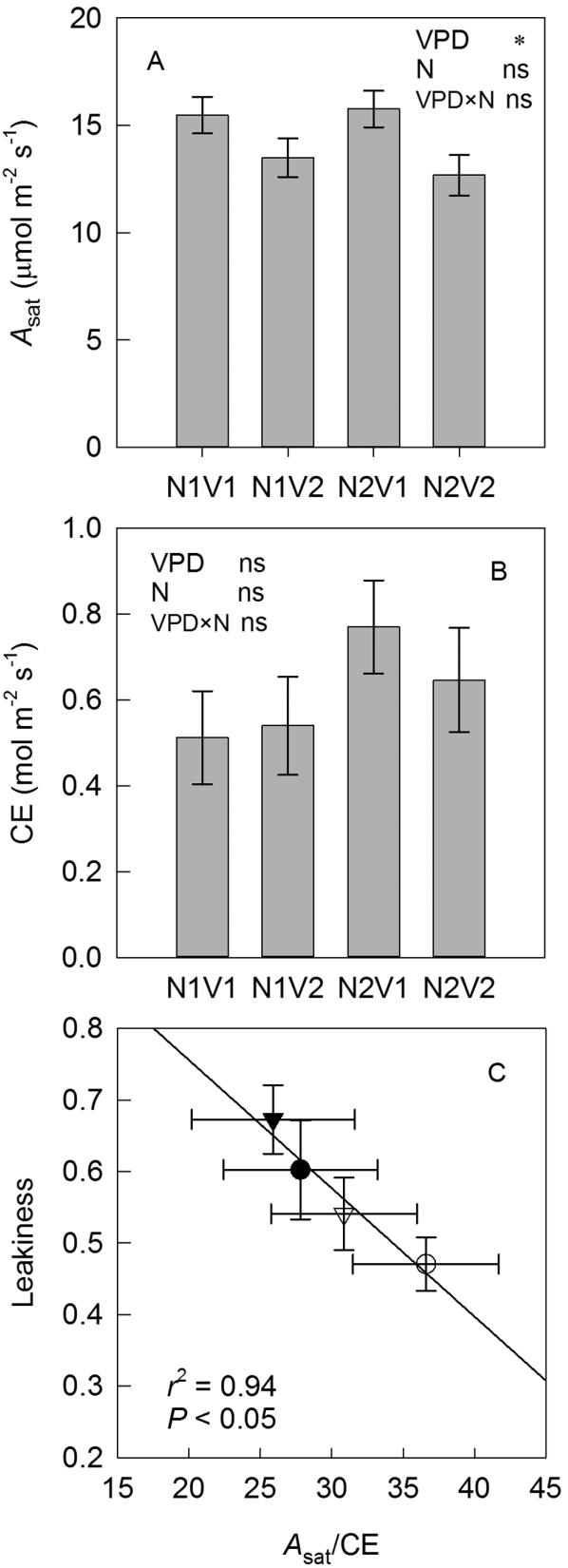

Fig. 4. A_{sat} (A), carboxylation efficiency (CE; B) and the relationship between leakiness measured under growth conditions (390 μmol mol^{-1}) and A_{sat}/CE (μmol mol^{-1}; C) under low or high N fertilizer supply (N1, circles; or N2, triangles) combined with low or high VPD (V1, open symbols; or V2, filled symbols). Data are shown as the mean±SE (n=9–10 for A_{sat} and CE, n=5–6 for leakiness). * indicates the treatment effect was significant at the P-level of 0.05, while ns indicates no significant effect.

influenced by VPD. The long-term response of leakiness to VPD was related to the decrease of C_i/C_a and the increase of Δ (0.55‰ at ambient CO_2 level) at high VPD, although the direct and indirect influences cannot be clearly distinguished due to the intrinsic correlation between C_i/C_a and Δ. The latter observation was also supported by the ^{13}C discrimination of leaf dry mass, which was significantly higher at high VPD (5.0±0.2‰, averaged over N levels) than at low VPD treatment (4.4±0.2‰). Likely, the higher leakiness at high VPD resulted from an enhanced capacity of the C_4 cycle relative to the C_3 cycle at low g_s, as was supported by the lower A_{sat}/CE ratio and the lower C_i/C_a at high VPD relative to low VPD. This interpretation is in line with the findings that the relative activities of Rubisco/PEPc decreased at low g_s under water stress, with the adjustment achieved by increasing activity of PEPc (Saliendra *et al.*, 1996; Foyer *et al.*, 1998) or decreasing sensitivity of PEPc to the inhibitor malate (Foyer *et al.*, 1998). Also, the data may shed light on the mechanism that underlies the increased leakiness under limited water supply (Saliendra *et al.*, 1996; Williams *et al.*, 2001; Fravolini *et al.*, 2002): that response may have been triggered by decreased stomatal conductance at high VPD. Although a VPD effect on this relationship has not yet been reported, the adjustment of Rubisco/PEPc activities seems to be an important mechanism for plants to counteract the reduced g_s under long-term low water supply (Saliendra *et al.*, 1996) or high VPD. Maintaining a powerful C_4 pump (at the expense of increased leakiness) might reduce the quantum yield due to the additional ATP requirement for PEP regeneration (Hatch, 1987; Furbank *et al.*, 1990). However, this mechanism may be beneficial for plants to maintain a high WUE_i under high VPD or drought stress.

In this work, high N nutrition increased leakiness in short-term exposures to subambient to ambient [CO_2], but not to elevated [CO_2] of 800 μmol mol^{-1}. This result is at variance with previous reports of a higher leakiness of plants growing with a low N supply (Meinzer and Zhu, 1998; Fravolini *et al.*, 2002). Other studies also reported non-significant effects of N supply on leakiness (Fravolini *et al.*, 2002; Wang *et al.*, 2012). In the present study, the plants of the low N treatment had a nitrogen nutrition index of ~0.8, which indicated that N was just growth limiting. High N supply led to a NNI of 1.3, and increased plant growth rate via stimulated tiller production (data not shown), but leaf-level net assimilation rates of young leaves were not affected. These results indicate that our low N and high N treatment represented rather 'nearly-adequate' and 'copious supply' of N for leaf-level photosynthesis. High N supply increased leakiness, in correspondence with a lower A_{sat}/CE ratio, again indicating the involvement of the relative activities of Rubisco/PEPc. This interpretation was further supported by the positive correlation between N_{mass} and CE, and simultaneous absence of such a relationship between N_{mass} and A_{sat}. These results suggest that under copious N supply to *C. squarrosa*, the activity of PEPc was more strongly enhanced relative to that of Rubisco, in line with experimental results on *Amaranthus retroflexus* (Sage *et al.*, 1987). Thus, our results are also in agreement with the hypothesis that C_4 plants have less plasticity in increasing the

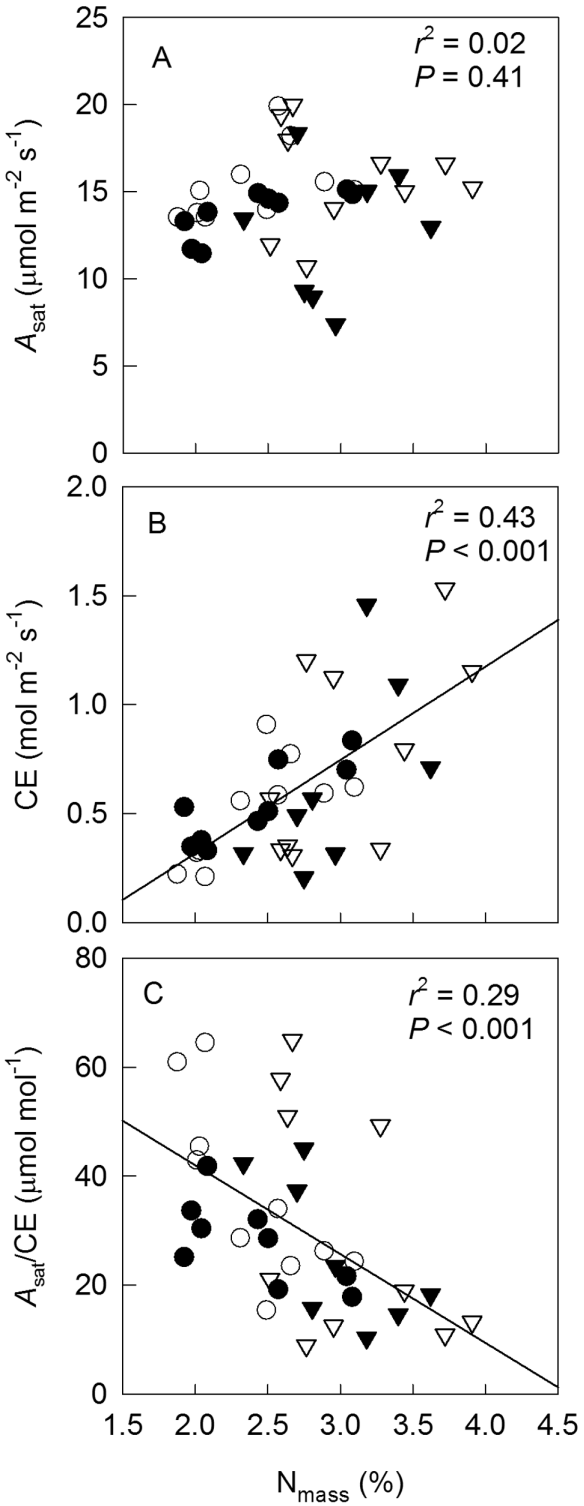

Fig. 5. Correlations between N_{mass} and A_{sat} (A), CE (B) and A_{sat}/CE (C) of leaves grown at low or high N fertilizer supply (N1, circles; or N2, triangles) combined with low or high VPD (V1, open symbols; or V2, filled symbols). Each symbol represents a data point of an individual plant.

amount of Rubisco compared with C_3 plants, due to spatial restrictions in bundle-sheath cells (Sage and McKown, 2006).

Another potential origin of the variance in leakiness is related to the bundle-sheath conductance ($g_{bs}=\phi V_P/(C_{bs}-C_m)$). However, current understanding on g_{bs} is limited due to the lack of a methodology for quantification of g_{bs} that is independent of gas exchange measurements. Furthermore, it is unknown how VPD may affect the properties of bundle-sheath cell walls, limiting to some extent discussions of potential mechanisms. A recent study demonstrated that *Miscanthus×giganteus* plants grown at high N supply had higher bundle-sheath area per unit leaf area, which might increase g_{bs}; however, estimates of leakiness did not differ between N levels (Ma *et al.*, 2016). Such results highlight the potential complexity of influences on leakiness by biochemical/physiological and anatomical features. In our study, treatments had little effect on individual leaf area and no effect on thickness (Liu *et al.*, 2016), indicating that effects of leaf anatomy may have been minor. Across all treatments, leakiness measured under growth conditions was negatively related to A_{sat}/CE, again suggesting that variations of leakiness across treatments was related to the balance between C_3 and C_4 cycles.

Response of bundle-sheath leakiness to short-term variation of CO_2

The response of ϕ to short-term variation of [CO_2] has been predicted by model analyses (von Caemmerer and Furbank, 1999; Kiirats *et al.*, 2002; Ghannoum, 2009; Yin *et al.*, 2011). Although these models were designed for estimating gas exchange rate rather than leakiness, the present results supported the theoretical predictions. So far, only a small number of studies investigated the response of ϕ to dynamic changes of [CO_2]. A study using the on-line Δ method showed no response of ϕ of *F. bidentis* to dynamic changes of CO_2 (Pengelly *et al.*, 2012), in agreement with the finding of an earlier study on several species (Henderson *et al.*, 1992). However, in the latter study, each leaf was measured at only two or three levels of CO_2. Those results suggested a rapid regulation of C_3 and C_4 cycle rates in response to changing CO_2 concentrations. The present results indicate that this kind of regulation did not occur to the same extent during short-term CO_2 responses in *C. squarrosa*. Clearly, the response of ϕ to short-term variation of CO_2 should be studied in detail with a greater number of species.

Implications on the ecophysiology of C. squarrosa

This work questions the interpretation of leakiness as a simple indicator for efficiency of C_4 photosynthesis or physiological fitness of C_4 plants, as increased leakiness was related to the enhancement of WUE_i in *C. squarrosa*. The latter observation was consistent across N and VPD treatments (long-term response) and short-term variation of CO_2 levels. This result was in line with the theoretical prediction of the simplified model of C_4 discrimination: WUE_i is positively correlated to leakiness when Δ>4.4‰, i.e. when ϕ>0.37. This relationship indicates a potential trade-off between quantum yield and water use efficiency: high leakiness under VPD stress might decrease the efficiency of energy use, but may be a condition for maintaining the effectiveness of CCM and minimizing photorespiration at a very low g_s in this species. This mechanism is meaningful for C_4 species in arid or semi-arid grasslands, where shading is uncommon but high VPD or drought

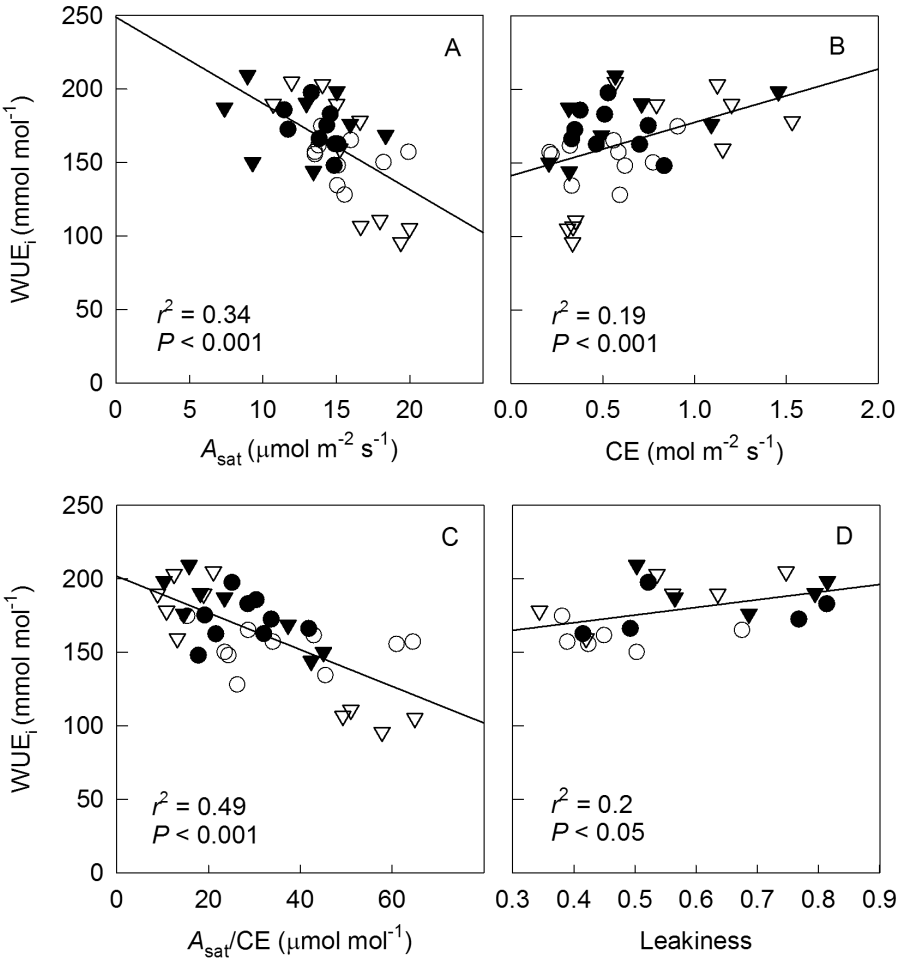

Fig. 6. Correlations between WUE_i and A_{sat} (A), CE (B), A_{sat}/CE (C), and leakiness (D) of leaves grown at low or high N fertilizer supply (N1, circles; or N2, triangles) combined with low or high VPD (V1, open symbols; or V2, filled symbols). Each symbol represents a data point of an individual plant.

stress is a common attribute of the habitat. Considering the reduction of Rubisco specificity for CO_2 relative to O_2 by the increase of leaf temperature, this trade-off may be important for C_4 plants in the context of global warming. Observational evidence has indeed shown that this C_4 grass has increased its relative abundance in vast areas of Inner Mongolian grasslands during regional warming in the last decades (Wittmer *et al.*, 2010).

Supplementary data

Supplementary data are available at *JXB* online.

Fig. S1. Relative humidity and leaf-to-air vapour pressure deficit in the leaf cuvette during the measurement of CO_2 response curves.

Fig. S2. Minimum mesophyll conductance to CO_2 (g_{mmin}=A/C_i) and estimated g_m in response to C_i.

Fig. S3. Photosynthetic light response curves of leaves of *C. squarrosa*.

Fig. S4. V_p and V_c in response to C_i.

Fig. S5. Bundle-sheath leakiness in response to C_i, calculated using different models of ^{13}C discrimination.

Fig. S6. Correlations between WUE_i and bundle-sheath leakiness of *C. squarrosa*.

Acknowledgements

This research was funded by the Deutsche Forschungsgemeinschaft (DFG SCHN 557/7-1). Wolfgang Feneis and Richard Wenzel are thanked for assistance with technical facilities. We thank Prof. von Caemmerer and two anonymous referees for constructive comments and suggestions that helped us to improve this work.

References

Barbour MM, Evans JR, Simonin KA, von Caemmerer S. 2016. Online CO_2 and H_2O oxygen isotope fractionation allows estimation of mesophyll conductance in C_4 plants, and reveals that mesophyll conductance decreases as leaves age in both C_4 and C_3 plants. New Phytologist **210,** 875–889.

Bellasio C, Griffiths H. 2014. Acclimation to low light by C_4 maize: implications for bundle sheath leakiness. Plant, Cell and Environment **37,** 1046–1058.

Berenson ML, Levine DM, Goldstein M. 1983. Intermediate statistical methods and applications: A computer package approach. Englewood Cliffs, NJ: Prentice-Hall.

Cousins AB, Badger MR, von Caemmerer S. 2008. C_4 photosynthetic isotope exchange in NAD-ME- and NADP-ME-type grasses. Journal of Experimental Botany **59,** 1695–1703.

Ehleringer JR, Cerling TE, Helliker BR. 1997. C_4 photosynthesis, atmospheric CO_2, and climate. Oecologia **112,** 285–299.

Elsig J, Leuenberger MC. 2010. ^{13}C and ^{18}O fractionation effects on open splits and on the ion source in continuous flow isotope ratio mass spectrometry. Rapid Communications in Mass Spectrometry **24,** 1419–1430.

Evans JR, Sharkey TD, Berry JA, Farquhar GD. 1986. Carbon isotope discrimination measured concurrently with gas-exchange to investigate CO_2 diffusion in leaves of higher plants. Australian Journal of Plant Physiology **13,** 281–292.

Farquhar GD. 1983. On the nature of carbon isotope discrimination in C_4 species. Australian Journal of Plant Physiology **10,** 205–226.

Farquhar GD, Cernusak LA. 2012. Ternary effects on the gas exchange of isotopologues of carbon dioxide. Plant, Cell and Environment **35,** 1221–1231.

Farquhar GD, Richards RA. 1984. Isotopic composition of plant carbon correlates with water-use efficiency of wheat genotypes. Australian Journal of Plant Physiology **11,** 539–552.

Flexas J, Ribas-Carbo M, Diaz-Espejo A, Galmes J, Medrano H. 2008. Mesophyll conductance to CO_2: current knowledge and future prospects. Plant, Cell and Environment **31,** 602–621.

Foyer CH, Valadier MH, Migge A, Becker TW. 1998. Drought-induced effects on nitrate reductase activity and mRNA and on the coordination of nitrogen and carbon metabolism in maize leaves. Plant Physiology **117,** 283–292.

Fravolini A, Williams DG, Thompson TL. 2002. Carbon isotope discrimination and bundle sheath leakiness in three C_4 subtypes grown under variable nitrogen, water and atmospheric CO_2 supply. Journal of Experimental Botany **53,** 2261–2269.

Furbank RT, Jenkins CLD, Hatch MD. 1990. C_4 photosynthesis: quantum requirement, C_4 and overcycling and *Q*-cycle involvement. Australian Journal of Plant Physiology **17,** 1–7.

Ghannoum O. 2009. C_4 Photosynthesis and water stress. Annals of Botany **103,** 635–644.

Ghashghaie J, Badeck F-W, Lanigan G, Nogués S, Tcherkez G, Deléens E, Cornic G, Griffiths H. 2003. Carbon isotope fractionation during dark respiration and photorespiration in C_3 plants. Phytochemistry Reviews **2,** 145–161.

Gong XY, Chen Q, Lin S, Brueck H, Dittert K, Taube F, Schnyder H. 2011. Tradeoffs between nitrogen- and water-use efficiency in dominant species of the semiarid steppe of Inner Mongolia. Plant and Soil **340,** 227–238.

Gong XY, Schäufele R, Feneis W, Schnyder H. 2015. $^{13}CO_2/^{12}CO_2$ exchange fluxes in a clamp-on leaf cuvette: disentangling artefacts and flux components. Plant, Cell and Environment **38,** 2417–2432.

Gresset S, Westermeier P, Rademacher S, Ouzunova M, Presterl T, Westhoff P, Schön CC. 2014. Stable carbon isotope discrimination is under genetic control in the C_4 species maize with several genomic regions influencing trait expression. Plant Physiology **164,** 131–143.

Hatch MD. 1987. C_4 photosynthesis: a unique blend of modified biochemistry, anatomy and ultrastructure. Biochimica et Biophysica Acta **895,** 81–106.

Henderson SA, von Caemmerer S, Farquhar GD. 1992. Short-term measurements of carbon isotope discrimination in several C_4 species. Australian Journal of Plant Physiology **19,** 263–285.

Henderson SA, von Caemmerer S, Farquhar GD, Wade L, Hammer H. 1998. Correlation between carbon isotope discrimination and transpiration efficiency in lines of the C_4 species *Sorghum bicolor* in the glasshouse and the field. Australian Journal of Plant Physiology **25,** 111–123.

Kiirats O, Lea PJ, Franceschi VR, Edwards GE. 2002. Bundle sheath diffusive resistance to CO_2 and effectiveness of C_4 photosynthesis and refixation of photorespired CO_2 in a C_4 cycle mutant and wild-type *Amaranthus edulis*. Plant Physiology **130,** 964–976.

Kromdijk J, Griffiths H, Schepers HE. 2010. Can the progressive increase of C_4 bundle sheath leakiness at low PFD be explained by incomplete suppression of photorespiration? Plant, Cell and Environment **33,** 1935–1948.

Lanigan GJ, Betson N, Griffiths H, Seibt U. 2008. Carbon isotope fractionation during photorespiration and carboxylation in *Senecio*. Plant Physiology **148,** 2013–2020.

Lehmeier CA, Lattanzi FA, Schäufele R, Wild M, Schnyder H. 2008. Root and shoot respiration of perennial ryegrass are supplied by the same substrate pools: assessment by dynamic ^{13}C labeling and compartmental analysis of tracer kinetics. Plant Physiology **148,** 1148–1158.

Lemaire G, Jeuffroy MH, Gastal F. 2008. Diagnosis tool for plant and crop N status in vegetative stage theory and practices for crop N management. European Journal of Agronomy **28,** 614–624.

Liu HT, Gong XY, Schäufele R, Yang F, Hirl RT, Schmidt A, Schnyder H. 2016. Nitrogen fertilization and $\delta^{18}O$ of CO_2 have no effect on ^{18}O-enrichment of leaf water and cellulose in *Cleistogenes squarrosa* (C_4) – is VPD the sole control? Plant, Cell and Environment, DOI: 10.1111/pce.12824.

Long SP. 1999. Environmental responses. In: Sage RF, Monson RK, eds. C_4 plant biology. San Diego: Academic Press, 215–249.

Ma J, Sun W, Koteyeva NK, Voznesenskaya E, Stutz SS, Gandin A, Smith-Moritz AM, Heazlewood JL, Cousins AB. 2016. Influence of light and nitrogen on the photosynthetic efficiency in the C4 plant *Miscanthus* × *giganteus*. Photosynthesis Research, DOI: 10.1007/s11120-016-0281-7.

Meinzer F, Zhu J. 1998. Nitrogen stress reduces the efficiency of the C_4 CO_2 concentrating system, and therefore quantum yield, in *Saccharum* (sugarcane) species. Journal of Experimental Botany **49,** 1227–1234.

Osborn HL, Alonso-Cantabrana H, Sharwood RE, Covshoff S, Evans JR, Furbank RT, von Caemmerer S. 2016. Effects of reduced carbonic anhydrase activity on CO_2 assimilation rates in *Setaria viridis*: a transgenic analysis. Journal of Experimental Botany, DOI: 10.1093/jxb/erw357.

Pengelly JJL, Sirault XRR, Tazoe Y, Evans JR, Furbank RT, von Caemmerer S. 2010. Growth of the C_4 dicot *Flaveria bidentis*: photosynthetic acclimation to low light through shifts in leaf anatomy and biochemistry. Journal of Experimental Botany **61,** 4109–4122.

Pengelly JJL, Tan J, Furbank RT, von Caemmerer S. 2012. Antisense reduction of NADP-malic enzyme in *Flaveria bidentis* reduces flow of CO_2 through the C_4 cycle. Plant Physiology **160,** 1070–1080.

Pyankov VI, Gunin PD, Tsoog S, Black CC. 2000. C_4 plants in the vegetation of Mongolia: their natural occurrence and geographical distribution in relation to climate. Oecologia **123,** 15–31.

Rogers A. 2014. The use and misuse of $V_{c,max}$ in Earth System Models. Photosynthesis Research **119,** 15–29.

Sage RF, McKown AD. 2006. Is C_4 photosynthesis less phenotypically plastic than C_3 photosynthesis? Journal of Experimental Botany **57,** 303–317.

Sage RF, Pearcy RW, Seemann JR. 1987. The nitrogen use efficiency of C_3 and C_4 Plants III. Leaf nitrogen effects on the activity of carboxylating enzymes in *Chenopodium album* (L) and *Amaranthus retroflexus* (L). Plant Physiology **85,** 355–359.

Saliendra NZ, Meinzer FC, Perry M, Thom M. 1996. Associations between partitioning of carboxylase activity and bundle sheath leakiness to CO_2, carbon isotope discrimination, photosynthesis, and growth in sugarcane. Journal of Experimental Botany **47,** 907–914.

Schnyder H, Schäufele R, Lötscher M, Gebbing T. 2003. Disentangling CO_2 fluxes: direct measurements of mesocosm-scale natural abundance $^{13}CO_2/^{12}CO_2$ gas exchange, ^{13}C discrimination, and labelling of CO_2 exchange flux components in controlled environments. Plant, Cell and Environment **26,** 1863–1874.

Ubierna N, Sun W, Cousins AB. 2011. The efficiency of C_4 photosynthesis under low light conditions: assumptions and calculations with CO_2 isotope discrimination. Journal of Experimental Botany **62,** 3119–3134.

Ubierna N, Sun W, Kramer DM, Cousins AB. 2013. The efficiency of C_4 photosynthesis under low light conditions in *Zea mays*, *Miscanthus* x *giganteus* and *Flaveria bidentis*. Plant, Cell and Environment **36,** 365–381.

von Caemmerer S, Furbank RT. 1999. Modeling C_4 photosynthesis. In: Sage RF, Monson RK, eds. C_4 plant biology. San Diego: Academic Press, 173–211.

von Caemmerer S, Ghannoum O, Pengelly JJL, Cousins AB. 2014. Carbon isotope discrimination as a tool to explore C_4 photosynthesis. Journal of Experimental Botany **65,** 3459–3470.

Wang ZC, Kang SZ, Jensen CR, Liu FL. 2012. Alternate partial root-zone irrigation reduces bundle-sheath cell leakage to CO_2 and enhances photosynthetic capacity in maize leaves. Journal of Experimental Botany **63,** 1145–1153.

Watling JR, Press MC, Quick WP. 2000. Elevated CO_2 induces biochemical and ultrastructural changes in leaves of the C_4 cereal sorghum. Plant Physiology **123,** 1143–1152.

Williams DG, Gempko V, Fravolini A, Leavitt SW, Wall GW, Kimball BA, Pinter PJ Jr, LaMorte R, Ottman M. 2001. Carbon isotope discrimination by *Sorghum bicolor* under CO_2 enrichment and drought. New Phytologist **150,** 285–293.

Wittmer MHOM, Auerswald K, Bai Y, Schäufele R, Schnyder H. 2010. Changes in the abundance of C_3/C_4 species of Inner Mongolia

grassland: evidence from isotopic composition of soil and vegetation. Global Change Biology **16,** 605–616.

Yang H, Auerswald K, Bai Y, Wittmer MHOM, Schnyder H. 2011. Variation in carbon isotope discrimination in *Cleistogenes squarrosa* (Trin.) Keng: patterns and drivers at tiller, local, catchment, and regional scales. Journal of Experimental Botany **62,** 4143–4152.

Yang F, Gong XY, Liu HT, Schäufele R, Schnyder H. 2016*a*. Effects of nitrogen and vapour pressure deficit on phytomer growth and development in a C_4 grass. AoB Plants, doi: 10.1093/aobpla/plw075.

Yang Z, Liu J, Tischer SV, Christmann A, Windisch W, Schnyder H, Grill E. 2016*b*. Leveraging abscisic acid receptors for efficient water use in *Arabidopsis*. Proceedings of the National Academy of Sciences of the United States of America **113,** 6791–6796.

Yin XY, Sun ZP, Struik PC, Van der Putten PEL, Van Ieperen W, Harbinson J. 2011. Using a biochemical C_4 photosynthesis model and combined gas exchange and chlorophyll fluorescence measurements to estimate bundle-sheath conductance of maize leaves differing in age and nitrogen content. Plant, Cell and Environment **34,** 2183–2199.